Proceedings of the
International Conference on Mechanical Engineering 2011
(ICME2011) 18-20 December 2011, Dhaka, Bangladesh

ICME11-FL-015

EFFECTS OF SIDE MASS INJECTION VELOCITY, LOCATION AND INLET SWIRL ON THE MAIN TURBULENT FLUID FLOW THROUGH A CIRCULAR DUCT

Snehamoy Majumder and Debajit Saha

Department of Mechanical Engineering, Jadavpur University, INDIA.

ABSTRACT

A numerical study is presented for the mixing of turbulent fluid injected at an angle of 45°and 90°with the horizontal direction into main turbulent bulk flow in an axi- symmetric circular duct. The analysis of the turbulent fluid flow through a circular duct having axial symmetry with side wall mass injection and inlet swirl have been carried out using modified $k-\varepsilon$ model, considering streamline curvature effects by modifying the model constants. The variation of the flow pattern of the turbulent fluid flow has been thoroughly investigated by varying the side mass injection velocity, the axial extent and position of the side injection site. The swirl number has been varied to analyze the effect of swirl, imparted at the inlet of the duct, on the flow pattern of the turbulent flow. Due to the side mass injection the recirculation bubble is formed at various location of the duct and the variation of the onset and size of the recirculation has been shown by vectors plotting along with the streamline contours.

Keywords: Side Mass Injection, Streamline Curvature, Modified $k-\varepsilon$ model, Swirl

1. INTRODUCTION

The side mass flow is injected normal to or at an angle with the axial direction of the duct into the main turbulent bulk flow in various industrial processes. In a gas turbine combustor, mixing of relatively cold air jets is important in the dilution zone where the products of combustion are mixed with the air to reduce the gas temperature acceptable to the turbine blade material in different radial locations. In General, the position, size and injection velocity of side jets greatly influence the performance of the combustor. The side injection is employed in a main turbulent fluid flow for the enhancement and control of the mixing operation, required for the stabilization of the combustion flame by the presence of the recirculation bubble generated.

The swirling flow is commonly applied in combustion systems and chemical processing plants, in order to increase the fluid mixing, heat and mass transfer rates and thus subsequently to improve the efficiency or the degree of stability of the process. The complete combustion of the fuel in the combustor is not only significant for obtaining high performance rating but also for minimizing the formation of carbon particles. These carbon particles are harmful for both the environment and combustion chamber. In order to maintain good turbulent mixing and high combustion efficiency there is necessity for the development of the recirculation zone in the combustor to prevent the flame of the combustor from being blown out and destabilized. To improve the flame stabilization and promote the mixing between the incoming fuel and the hot products of combustion the swirl is imparted to the incoming combustion air prior to the entry into the primary zone. The degree of the influence of swirling flow is usually characterized by the swirling number, which is a non dimensional number. In the present analysis the effect of the swirl on the flow field has been observed.

Flow and heat transfer measurements were made in an annulus having a diameter ratio of 0.5 with injection at the inner tube by El-Nashar [1]. Due to the injection, the mean axial velocities near the porous tube gradually decreased and the position of maximum velocity shifted towards the outer tube. They also showed that the turbulent intensity and Reynolds stress near the porous wall increased due to injection.

A numerical study was presented by Chang and Chen [4] for the mixing of heated line jets discharged normally or at angle into a cold cross flow. They have used $\kappa-\varepsilon$ turbulence model and the angle has been varied from 60° to 90°. The results showed that a strong recirculation ahs been generated near the downstream region and better thermal mixing can be achieved at higher momentum

flux ratio and incident angle.

The effects of side inlet angle on mixing phenomena in a three dimensional side dump combustor have been numerically investigated by Ko [5]. The side inlet angle has been varied as 30°, 60° and 90° and the results showed that the recirculation structures and secondary flow motions along with the other flow features of the combustor are all significantly influenced by the variation of the side inlet angle.

Ting-ting and Shao-hua [6] numerically presented the mean velocity and kinetic energy fields for three dimensional lateral jets in cross flow at the injection angle of 60° and 30°. They showed that the affected zone by injected jets laterally increase at upstream with the increase of injection angle and jet to cross flow momentum ratio.

Salewski *et al.* [7] numerically and experimentally investigated the coherent structures and mixing in the flow field of a jet in a cross flow. The flow field of jet in cross flow is highly unsteady and has several typical and distinguishable structures. They analyzed the turbulent statistics and mean scalar fields for both the circular and non circular jets.

On the other hand, Tehrani and Feizollahi [8] numerically investigate the penetration and mixing characteristics of directly opposed rows of coolant jets injected normally into a heated confined cross stream. The effect of jet-to-mainstream momentum flux ratio was investigated. The result showed that with the increase of jet to crossflow momentum ratio and the periodic distance of the adjacent jets the jet penetration also increased.

The effects of side mass injection with centrally confined jet entry at inlet to a circular duct ahs been numerically investigated by Majumder and Sanyal [10]. The results showed that due to the side mass injection relaminarization of the turbulent flow can occur and the flow becomes stabilized. The variation of turbulent energy distribution, shear stress distribution and friction factor has been analyzed and the gradual decrease of these quantities with the increase of the injection velocity indicates the relaminarization of the flow.

Using the cooling air in the gas turbine combustor kamotani and Greber [12] studied the mixing operation of combustion gasses. They showed that the velocity distribution mainly depends on the jet to cross flow momentum flux whereas; the temperature distribution depends on the jet to crossflow density ratio. The results also showed that behind the jet, a pair of vortices generated and in the far downstream region these vortex structure becomes a dominant feature of jet.

Vranos *et al.* [13] experimentally investigated cross stream injection and mixing in a cylindrical duct by varying the momentum ratio, density ratio and injector geometry. They found that mixing rate decreases with increasing density ratio and above a certain momentum flux ratio, mixing is faster with slanted slot injectors than with round hole injectors.

Oechsle *et al.* [14] analytically studied the affects of jet to mainstream momentum flux ratio, orifice geometry, orifice orientation and the number of orifices on the mixing process of RQL combustor. They showed that the best mixing configuration depends on the penetration depth of the jet. The increase in the number of orifices per row increases the mixing process but at a higher momentum ratio it has an adverse affect due to the formation of strong swirl at the mixing region.

In the present study, a numerical analysis of the turbulent fluid flow through a circular duct having axial symmetry with side wall mass injection and inlet swirl have been carried out considering the angle of injection as 45°and 90°. Standard k -ε model together with modification due to streamline curvature has been employed to resolve the re-circulating flow regions accurately. The modification used by Majumder and Sanyal [9] has been employed and implemented in the present study to predict the effect of the streamline curvature. The flow has been considered to be incompressible, steady, turbulent, nonreacting and axi-symmetric. The control volume formulation with power law scheme of S. V. Patankar [11] with SIMPLER algorithm has been adopted. The momentum and the k -e equations have been solved with the aid of standard wall function. It has been observed that the onset of recirculation as well as length and breadth of the recirculation bubble strongly depends on the side injection.

2. GEOMETRICAL DESCRIPTION

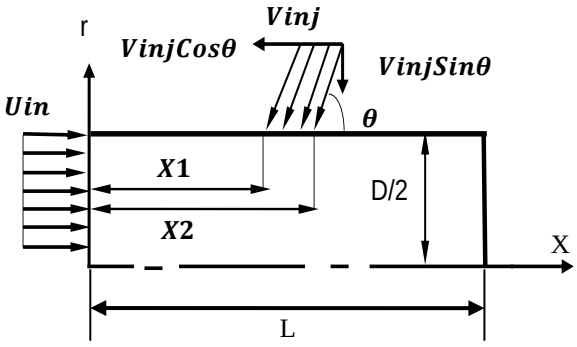

Fig 1. Schematic diagram of the axi-symmetric circular duct with main turbulent flow and angular side injection (θ= 45°and 90°)

Fig. 1 shows the uniform fluid flow through the axi-symmetric circular duct with side injection at a certain angle with the upstream direction. Here, the side injection angle is considered as 45° and 90°. In this case cylindrical co-ordinate $r - x$ has been considered. Here, inlet fluid flow is shown by U_{in} and the side injection is given by V_{inj}. The angle of side injection is given by θ. When the side injection is at an angle of θ with the cylindrical wall, the side injection can be resolved into two components. These two components are V_{inj} Sin θ and V_{inj} Cos θ. The axial extent of side injection is from X_1 to X_2. The length of the duct is represented as L.

For the present investigation the following nomenclature has been taken,

The axial length of the duct is considered as L = 9 m.

The diameter of the duct is considered as D= 0.1534 m.

Air density, ρ=1.235 kg/m^3.

Molecular viscosity of air, μ_l=1.853×10^{-5}kg/m.s.

Reynolds number, $Re = (\rho U_{mean} D)/\mu_l$. where U_{mean} is the mass-averaged axial inlet velocity.

3. MATHEMATICAL FORMULATION

The behavior of the flow is in general governed by the fundamental principles of classical mechanics expressing the conservation of mass, momentum and passive scalar. The mass conservation equation is required to compute the pressure field, after obtaining the velocity field from the momentum balance, and this is traditionally accomplished by via a staggered grid configuration.

Here, we consider steady, turbulent flows of an incompressible fluid modeled by the momentum and continuity equations.

3.1 Governing Equations

Continuity Equation:

$$\frac{\partial(\rho\bar{u})}{\partial x}+\frac{1}{r}\frac{\partial(\rho r\bar{v})}{\partial r}=0 \quad \textbf{(1)}$$

Momentum Equations:
Axial Component (x-component):

$$\rho\left[\bar{v}\frac{\partial\bar{u}}{\partial r}+\bar{u}\frac{\partial\bar{u}}{\partial x}\right]=-\frac{\partial\bar{p}}{\partial x}+\frac{\partial}{\partial x}\left(\mu_{eff}\frac{\partial\bar{u}}{\partial x}\right)+\frac{1}{r}\frac{\partial}{\partial r}\left(r\mu_{eff}\frac{\partial\bar{u}}{\partial r}\right)+\left[\frac{\partial}{\partial x}\left(\mu_{eff}\frac{\partial\bar{u}}{\partial x}\right)+\frac{1}{r}\frac{\partial}{\partial r}\left(r\mu_{eff}\frac{\partial\bar{v}}{\partial x}\right)\right] \quad \textbf{(2)}$$

Radial Component (r-component):

$$\rho\left[\bar{v}\frac{\partial\bar{v}}{\partial r}+\bar{u}\frac{\partial\bar{v}}{\partial x}\right]=-\frac{\partial\bar{p}}{\partial r}+\frac{\partial}{\partial x}\left(\mu_{eff}\frac{\partial\bar{v}}{\partial x}\right)+\frac{1}{r}\frac{\partial}{\partial r}\left(r\mu_{eff}\frac{\partial\bar{v}}{\partial r}\right)+\left[\frac{\partial}{\partial x}\left(\mu_{eff}\frac{\partial\bar{u}}{\partial r}\right)+\frac{1}{r}\frac{\partial}{\partial r}\left(r\mu_{eff}\frac{\partial\bar{v}}{\partial r}\right)\right]-2\mu_{eff}\frac{\bar{v}}{r^2}+\rho\frac{\bar{w}^2}{r} \quad \textbf{(3)}$$

Tangential Component (Θ- component):

$$\rho\left[\bar{v}\frac{\partial\phi}{\partial r}+\bar{u}\frac{\partial\phi}{\partial x}\right]=-\frac{\partial\bar{p}}{\partial r}+\frac{\partial}{\partial x}\left(\mu_{eff}\frac{\partial\phi}{\partial x}\right)+\frac{1}{r}\frac{\partial}{\partial r}\left(r\mu_{eff}\frac{\partial\phi}{\partial r}\right)-\frac{2}{r}\left[\frac{\partial}{\partial r}\mu_{eff}\phi\right] \quad \textbf{(4)}$$

Where, $\bar{u},\bar{v}$ *and* $\bar{w}$ are the mean velocity components along X, r and θ directions respectively.

And the variable $\phi = r\bar{w}$.

The effective viscosity is,

$$\mu_{eff}=\mu_l+\mu_t \quad \textbf{(5)}$$

Where, μ_l and μ_t are molecular or laminar viscosity and eddy or turbulent viscosity respectively.

Equation (1), (2) and (3) are governing equations for describing the mean flow characteristics of a turbulent flow.

The eddy viscosity is given by,

$$\mu_t=\rho C_\mu k^2/\varepsilon$$

Where C_μ is an empirical coefficient.

According to the ref. [3] and ref. [9] the modification of the empirical constant is given by,

$$C_\mu=\frac{-K_1K_2}{\left[1+8K_1^2\frac{k^2}{\varepsilon^2}\left(\frac{\partial U_S}{\partial n}+\frac{U_S}{R_C}\right)\frac{U_S}{R_c}\right]} \quad \textbf{(6)}$$

Here, $U_S=\sqrt{\bar{u}^2+\bar{v}^2}$

R_C is the radius of curvature of the concerned streamline (ψ = constant). The detail of equation (5) is given by ref. [13] with K_1 and K_2 equal to 0.27 and 0.3334, respectively.

3.2 Turbulence $\kappa-\varepsilon$ Model

In equation (5) two unknowns are introduced and will require the solution of two partial differential equations for the turbulent kinetic energy and turbulent dissipation rate. This is why $\kappa-\varepsilon$ model is identified as a two-equation eddy viscosity model. One of these equations governs the distribution of turbulent energy κ throughout the field and the other equation governs the turbulence dissipation rate ε. The transport equations governing the turbulence properties are obtained from the Navier-Stokes equation.

The $\kappa-\varepsilon$ equations are given by,

$\kappa-$Equation:

$$\rho\left[\bar{u}\frac{\partial k}{\partial x}+\bar{v}\frac{\partial k}{\partial r}\right]=\frac{\partial}{\partial x}\left[\left(\mu_l+\frac{\mu_t}{\sigma_k}\right)\frac{\partial k}{\partial x}\right]+\frac{1}{r}\frac{\partial}{\partial r}\left[r\left(\mu_l+\frac{\mu_t}{\sigma_k}\right)\frac{\partial k}{\partial r}\right]+\rho G-\rho\varepsilon \quad \textbf{(7)}$$

Where, G is the production term and given by:

$$G=\mu_t\left[2\left\{\left(\frac{\partial\bar{v}}{\partial r}\right)^2+\left(\frac{\partial\bar{u}}{\partial x}\right)^2+\left(\frac{\bar{v}}{r}\right)^2\right\}+\left(\frac{\partial\bar{u}}{\partial r}+\frac{\partial\bar{v}}{\partial x}\right)^2\right] \quad \textbf{(8)}$$

$\varepsilon-$Equation:

$$\rho\left[\bar{u}\frac{\partial\varepsilon}{\partial x}+\bar{v}\frac{\partial\varepsilon}{\partial r}\right]=\frac{\partial}{\partial x}\left[\left(\mu_l+\frac{\mu_t}{\sigma_\varepsilon}\right)\frac{\partial\varepsilon}{\partial x}\right]+\frac{1}{r}\frac{\partial}{\partial r}\left[r\left(\mu_l+\frac{\mu_t}{\sigma_\varepsilon}\right)\frac{\partial\varepsilon}{\partial r}\right]+C_{\varepsilon1}G\frac{\varepsilon}{k}-C_{\varepsilon2}\frac{\varepsilon^2}{k} \quad \textbf{(9)}$$

Here, $C_{\varepsilon1}, C_{\varepsilon2}, \sigma_k$ and σ_ε are the empirical turbulence constants, and some typical values of these constants in the standard K-ε model are recommended by Launder and Spalding [2] which are given below-

$C_{\varepsilon 1}$ = 1.44

$C_{\varepsilon 2}$ = 1.92

σ_k = 1.0

σ_ε = 1.3

Two arrays of 201 X 101 and 501 X 201 grid points in axial and radial directions, respectively, have been used. It has been observed that the grid independent study has shown 0.001% change in the stream wise velocity change. However, for the sake of accuracy, the finer grid array of 501 X 201 has been used for all subsequent results reported here.

3.3. Swirl Number

The degree of the influence of swirling flow is usually characterized by the swirling number, which is a non-dimensional number. The swirl number is the ratio between the axial fluxes of the swirl momentum to the axial flux of the axial momentum.

$$S = \frac{\int_0^R \overline{U}\,\overline{W} r^2 dr}{R \int_0^R \overline{U}^2 r dr} \qquad \textbf{(10)}$$

Where, R is the radius of the pipe at different axial positions. $\overline{U}$ and $\overline{W}$ are the mean axial and tangential velocity components, respectively.

4. BOUNDARY CONDITIONS

The governing equations by themselves do not yield solution to the given problem. Therefore additional boundary information is required at the inlet, outlet, the axis and the solid wall.

At the Inlet

(a) The inlet axial velocity is uniform. (U_{in}= Constant)

(b) Fully developed velocity profile has been taken at the inlet.

At the Wall

(a) No slip wall boundary condition has been taken for the solid wall (u =0, v=0).

(b) Both *k* and ε are handled by the wall function.

At the Axis

Zero shear stress condition has been taken for the axis.

At the Outlet

Fully developed flow condition has been taken at the outlet.

4. RESULTS AND DISCUSSIONS

The variation of the side injection velocity, Inlet main fluid velocity, and side injection extent and side injection site location has been investigated for the side injection angle of 90° and 45°. The variation of the flow pattern has been compared by the flooded streamline contours and vector diagrams to analyze the effect of the above parameters.

4.1 Effects of Variation of Side Injection Velocity

Fig. 2 shows the flooded streamline contour along with the vector diagram with inlet uniform axial velocity U_{in} = 0.5 m/s. The ratio of side injection velocity to inlet velocity has been varied from 1.2 to 2.4 by increasing the side injection velocity from 0.1 m/s to 1.2 m/s. The side injection site has been located at 2% of the length of the duct whereas the extent of injection has been taken 1% of the length of the duct. Here the injection angle is 90^0. It is observed that with the increase of the side injection velocity the penetration depth gradually increases. When the injection velocity is 2 times of the inlet velocity a recirculation bubble appears at the upstream of the duct. When the side injection velocity is 1 m/s, the inlet fluid flow does not overcome the resistance offered by the side injected mass and there is a drop in pressure in the upstream side of the duct. The ultimate consequence is the generation of the recirculatory flow. With the increase of the injection velocity, the size of the recirculatory flow also increases. This is signifying that the more is the side injection velocity, the more will be the penetrating capability of the injected fluid through the main flow, which is flowing with a constant velocity.

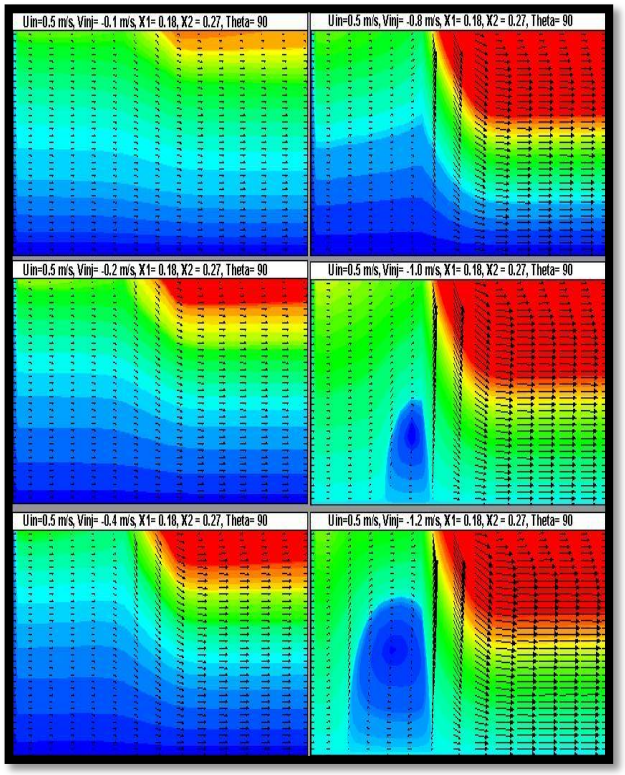

Fig 2. Effects of Injection Velocity on the Main Turbulent Fluid Flow (Injection Angle = 90°)

Fig. 3, shows the effect of injection velocity when the injection angle is 45^0. The other parametrs are same as before. From the fig. it has been observed that with the increase of the injection angle the penetration depth gradually increases. But in this case when the injection velocity is 1 m/s, no recirculation genetated at the upstream of the duct. So, it is observed that when the injection angle is 45^0, the resistance offred by the injected fluid to the main inlet flow is less in comparison to the earlier case. When the recirculation flow is needed at the upstream of duct at realtively lower velocity ratio of the injected fluid to the inlet fluid, the injection angle

should kept orthogonal to the streamwise direction.

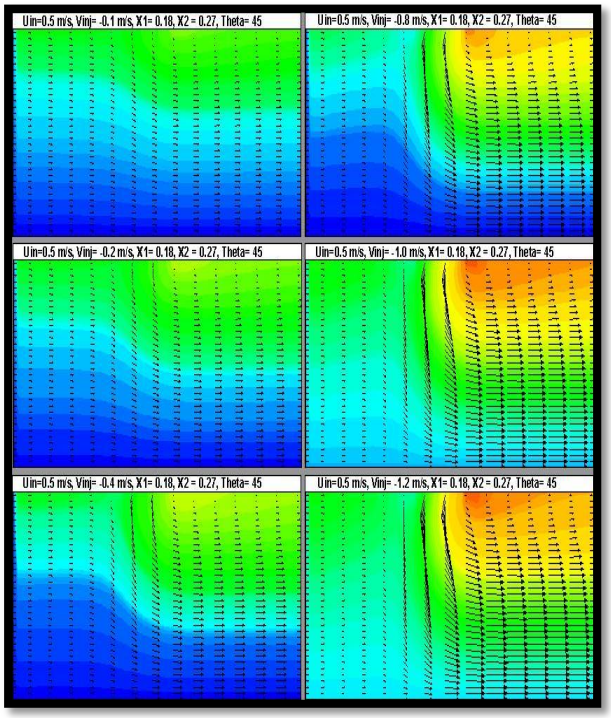

Fig 3. Effects of Injection Velocity on the Main Turbulent Fluid Flow (Injection Angle = 45°)

4.2 Effects of Variation of Inlet Fluid Velocity

Fig. 4 and fig. 5 shows the variation of the flow pattern of the turbulent flow with the variation of the inlet fluid velocity. In fig. 3, the injection angle is 90° and in fig. 4, the injection angle is 45°.

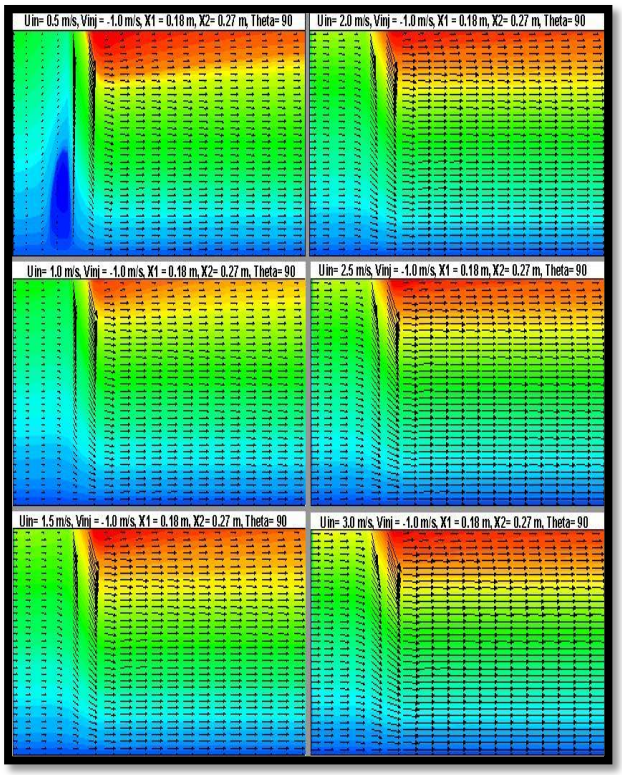

Fig.4, Effect of Inlet Fluid Flow Variation on the main Turbulent Fluid Flow (Injection Angle 90^0)

From both of the figures, it has been observed that with the increase of the inlet fluid velocity keeping the injection velocity constant, the penetration depth gradually decreses. From the fig. 3, it has been observed that when the injection angle is 1 m/s and inlet fluid velocity is 0.5 m/s, a recirculation is generated. When the inlet fluid velocity increases to 1 m/s, the recirculation vanishes and a recircualation free flow has been observed. And with further increse of the inlet fluid velocity decreses the penetration depth gradually. This is physically possible due to the fact that the momentum of the inlet main axial flow is increased due to the increase in axial velocity which forces the side injection flow not to penetrate further into the main flow. Thus the rapid mixing of the two cross flow has been observed to reduce by increasing the inlet velocity of the main flow. It definitely affects the flow pattern of the upstream side fluid motion in the cylindrical duct, since under such conditions the Entrance length usually increases.

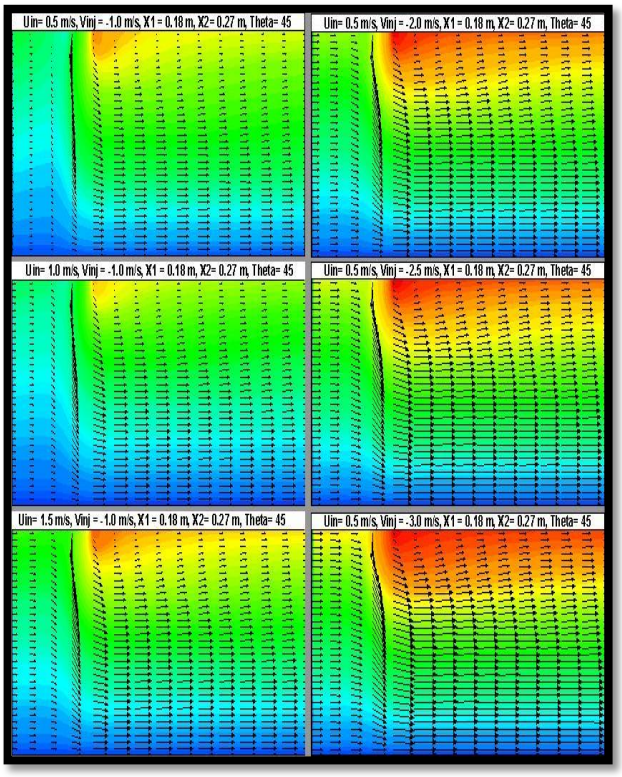

Fig 5. Effect of Inlet Fluid Flow Variation on the main Turbulent Fluid Flow (Injection Angle 45^0)

4.3 Effect of Variation of Axial Position of the Side Mass Injection Site

Fig. 6 and fig. 7 shows the variation of the flow pattern of the main turbulent fluid flow with the variation of the axial position of the side inejction site. The axial position of the injection site plays an important role in the variation of the flow pattern and the size of the recirculation formed at upstream. The inlet fluid velocity and the side inejction velocity has been kept as 0.5 m/s and 1.2 m/s respectively. The axial extent of side injection is 1% of the length of the duct. The side injection site has been located at a distance of 2% of the length of the duct and it has been gradually varied as 4%, 6%, 8%, 10% and 15% of the length of the duct. When

the injection angle is 90°, a recirculation is formed at the inlet of the duct when the injection site is being placed at 2% of the length of the duct. But when the side injection angle is 45°, the recirculatory flow generated when the injection site has been placed at 4% of the length of the duct.

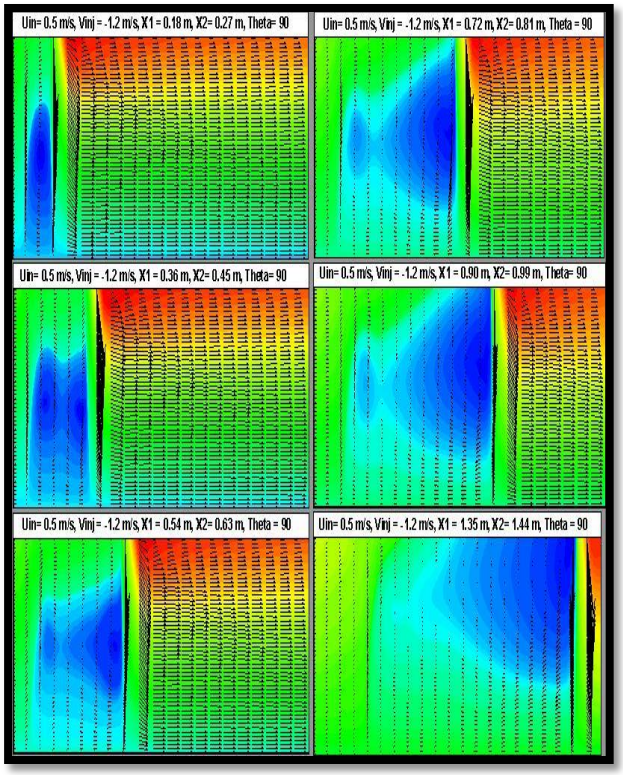

Fig 6. Effect of Variation of the Axial Position of Side injection Site (Injection Angle 90°)

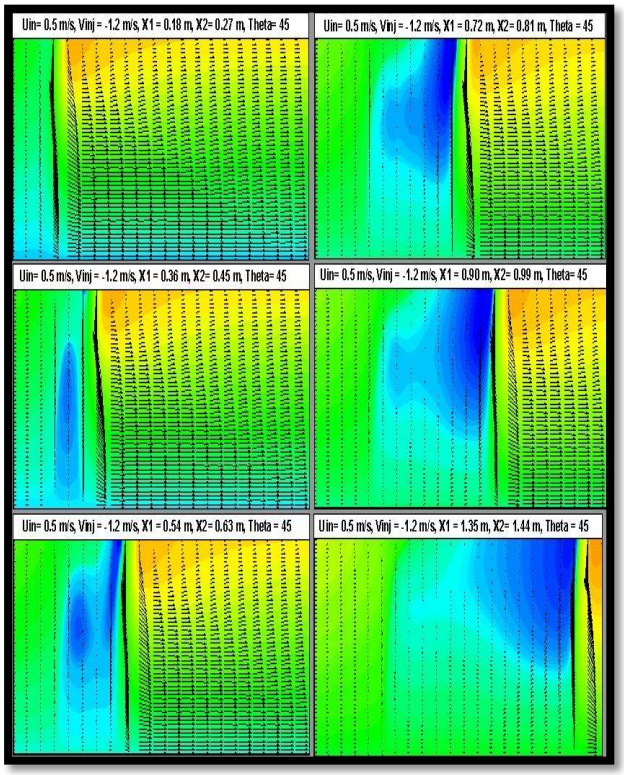

Fig 7. Effect of Variation of the Axial Position of Side injection Site (Injection Angle 45°)

From both of the figures it is evident that, with the relocation of the injection site towards downstream, the size of the recirculation generated at upstream gradually increases and the recirculation shifted towards the wall of the duct.

So, it can be said that to avoid the generation of the seceondary flow at axis of the duct the injection site should be relocated towards the downstream. But as the size of the recirulation gradually increases, so in case of gas turbine combustor, the local heating and Nox accumulation towards the wall also increases with the change in position of the injection site towards downstream.

4.4 Effects of Variation of Axial Extent of the Side Injection

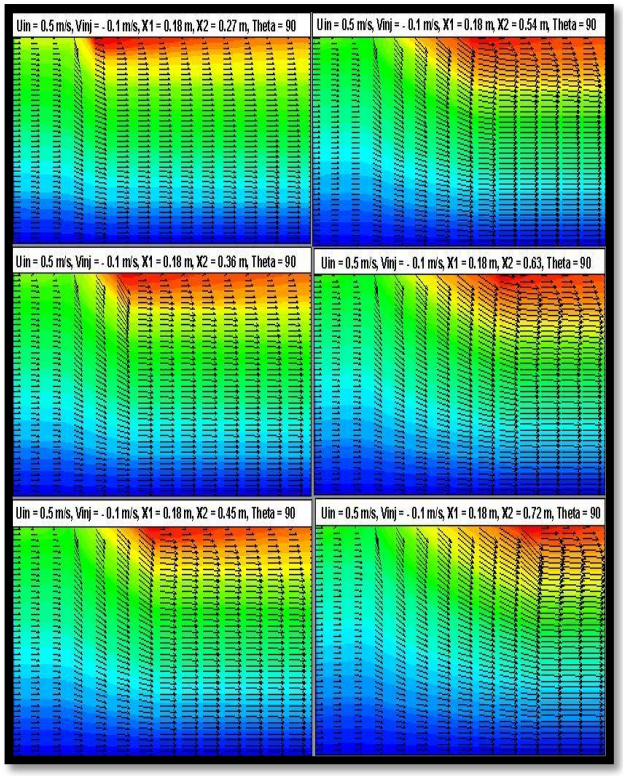

Fig 8. Effects of Variation of the Axial Extent of Side Injection (Injection Angle 90°)

Fig. 8 and fig. 9 shows the effects of the variation of axial extent of side injection on the flow pattern of the main turbulent fluid flow in the circular duct. The inlet fluid velocty and side injection velocity has been kept 0.5 m/s and 0.1 m/s respectively. The injection of the side mass has been started at a distance of 0.2% of the length of the duct and the extent of injection site has been gradually increased to analyze the effect of axial exetnt of injection on the flow patten.

In fig. 8, the injection angle is 90° and in fig.9, the inejction angle is 45°. The axial extent has been varied as 1%, 2%, 3%, 4%, 5% and 6% of the length of the duct. From both the figures it has been observed that with the increase of the axial extent, the penetration depth gradually increases As the area of injection increases, the momentum of the side injected mass also increases and a

larger mass of main flow comes under the perview of penetration.

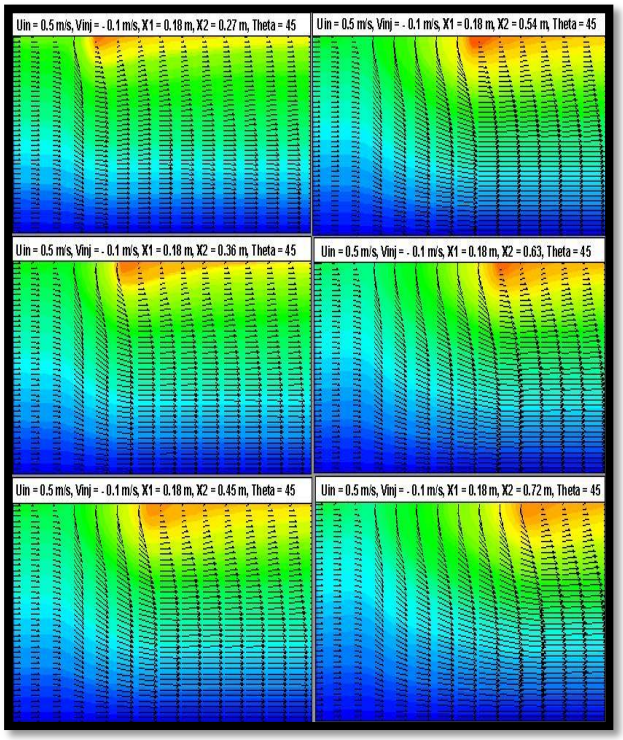

Fig 9. Effects of Variation of the Axial Extent of Side Injection (Injection Angle 45°)

4.4 Effect of Inlet Swirl

In fig. 10, the effect of swirl imparted at the inlet has been shown with flooded contour and vector diagram. The inlet velocity and side injection velocity has been kept as 0.5 m/s and 1.2 m/s respectively. The length of the cylindrical duct has been taken as 1 m. The side injection site has been located at a distance of 6% of the length of the duct and the injection width has been taken as 1% of the length of the duct. The swirl is created by introducing an external tangential velocity in azimuthal direction on the main turbulent flow at the inlet of the duct. From the fig., it is evident that with the increase of the swirl number, the size of the recirculation generated at the upstream gradually decreases and at a certain swirl number it almost disappears. From the diagram it is observed that the recirculation generated resides near the wall due to the side mass injection with and without any swirl. However due to the application of the swirl the size of the recirculation bubbles have been found to reduce with the increase of the swirl number and almost disappears at a swirl number of S =3.33.. In the flooded contour of the streamlines it is observed that the streamline pattern is indicating the residence of recirculation bubble near the wall and its strength is reducing by the application of the swirl imparted at the inlet. In this case the swirl is opposing the bubble generation and the flow is becoming less recirculatory. These results show that by increasing swirl number it is possible to prevent generation of recirculation bubble in the mixing region. This implies that by applying inlet swirl, we can control size of recirculation bubble caused by the side mass injection in the main turbulent bulk flow of the cylindrical duct. The swirl intensity suppresses the reversal stream wise velocity in magnitude at the identical locations indicating the effects of centrifugal force of the swirling fluids at the inlet side.

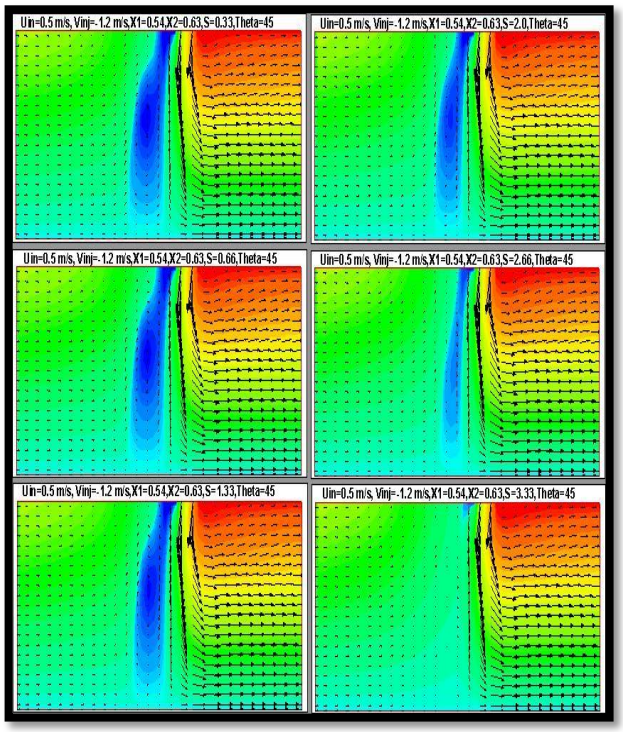

Fig 10. Effect of Inlet Swirl on the Main Turbulent Fluid Flow (Injection Angle 45^0)

5. CONCLUSION

The turbulent fluid flow through an axi-symmetric circular duct with side mass injection has been thoroughly investigated. The side mass injection plays an important role on flow pattern of the main turbulent flow in the circular duct. The principle conclusions from the numerical analysis summarized herein are:

1. The penetration depth of the side injection is dependent on the V_{inj}/U_{in} ratio and with the increase of the side injection velocity penetration depth increases whereas, it decreases with the increment of the inlet fluid velocity.
2. The penetration effect depends on the angle of the side injection as the penetartion depth is more when the side mass is injected orthogonally to the main duct fluid. When the injection angle is 45°, the recirculation is generated at upstream at a higher velocity ratio of the injected fluid to the inlet fluid.
3. The axial position of side injection site plays a vital role on the size of the recirculation generated in the duct. The recirculation size gradually increases with the increase of the distance of the injection site from the inlet of the duct and it shifts towards the wall from the axis.
4. The effect of side injection increases with the increase of the axial extent of side injection. A large mass of main fluid have been penetrated with a bigger extent of side mass injection.
5. It has been observed that using the swirling flow at the inlet could control the recirculation generated by the side mass injection at the wall region.

6. REFERENCES

1. El-Nashar, A.M., 1974, "Turbulent Flow in an Annulus with Injection: An Experimental Study", I*nd. Eng. Chem., Fundam.,* 13(1): pp. 33-38.
2. Launder, B. E. and Spalding, D. B., 1974, "The numerical computation of turbulent flows", *Computer Methods in Applied Mechanics*, 3: pp. 269-289.
3. Leschziner, M. A. and Rodi, W., 1981, "Calculation of Annular and Twin Parallel Jets Using Various Discretization Schemes and Turbulence-Model Variations", *Trans. ASME, J. Fluids Eng.,* 103: pp. 352-360.
4. Chang, Y.R. and Chen, K.S., 1995, "Prediction of Opposing Turbulent Line Jets Discharged Laterally into a Confined Cross Flow", *International Journal of Heat and Mass Transfer*, 38(9): pp. 1693-1703.
5. Ko, T.H., 2006, "A Numerical Study on the Effects of Side-Inlet Angle on the mixing Phenomena in a Three Dimensional Side –Dump Combustor", *International Communications in Heat and Mass Transfer*, 33: pp. 852-862.
6. Ting-ting, G. and Shao-hua, L., 2006, "Numerical Simulation of Turbulent Jets with Lateral Injection into a Cross Flow", *Journal of Hydrodynamics*, 18(3): pp. 319-323.
7. Salewski, M., Stankovic D. and Fuchs, L., 2008, "Mixing in Circular and Non-Circular Jets in Cross Flow", *Flow Turbulence Combust*, 80: pp. 255-283.
8. Tehrani, F.B. and Feizollahi, H., 2008, "Numerical Analysis of Opposed Rows of Coolant Jets Injected into a Heated Cross Flow", *IUST International Journal of Engineering Science,* 19: pp. 89-96.
9. Majumder S. and Sanyal D., 2008, "Destabilization of Laminar Wall Jet Flow and Re-Laminarization of the Turbulent Confined Jet Flow in Axially Rotating Circular Pipe", *Journal of Fluid Engineering, ASME,* 130(1): pp. 011203-1-011230-16.
10. Majumder S. and Sanyal D., 2010, "Relaminarization of Axi-symmetric Turbulent Flow with Combined Axial Jet and Side Injection in a Pipe", *Journal of Fluid Engineering, ASME*, 132(10): pp. 101101-1-101101-6.
11. Patankar, S. V., 1981, "Numerical Heat Transfer and Fluid Flow", *McGraw Hill, New York*.
12. Kamotani, Y. and Greber, I., 1974, "Experiments on Confined Turbulent Jets in Cross Flow", *NASA CR-2392*.
13. Vranos, A., Liscinsky, D.S., True, B. and Holdeman J.D., 1991, "Experimental Study of Cross Stream Mixing in a Cylindrical Duct", *NASA Technical Memorandum 105180, AIAA-91-2459*, Prepared for the 27th Joint Propulsion Conference, Sacramento, California.
14. Oechsle, V.L., Mongia, H.C. and Holdeman, J.D., 1992, "A Parametric Numerical Study of Mixingin a Cylindrical Duct", *NASA Technical Memorandum 105695, AIAA 92-3088*, Prepared for the 28th Joint Propulsion Conference and Exhibit, Nashvillie Tennessee.

7. NOMENCLATURE

Symbol	Meaning	Unit
D	Diameter of the cylindrical duct	(m)
L	Length of the cylindrical duct	(m)
R	Radius of the cylindrical duct	(m)
X	Axial co-ordinate along the duct	
r	Radial co-ordinate across the duct	
k	Turbulent kinetic energy	(m^2/s^2)
ε	Turbulent dissipation rate	(m^2/s^3)
ρ	Density of air	(kg/m^3)
$\bar{u}$	Time mean velocity along *x*-axis	(m/s)
$\bar{v}$	Time mean velocity along *y*-axis	(m/s)
μ	Viscosity of the air	(kg/m-s)
U_{mean}	Mass-averaged mean axial velocity	(m/s)
$\mathrm{R_e}$	Reynolds Number	($\rho vD/\mu$)
K_1	Constant	
K_2	Constant	
θ	Angle of Injection	Degree, °
U_{in}	Inlet Flow Velocity	(m/s)
V_{inj}	Side Injection Velocity	(m/s)
μ_l	Laminar Viscosity	(kg/m-s)
μ_t	Eddy Viscosity	(kg/m-s)
μ_{eff}	Effective Viscosity	(kg/m-s)
C_μ	Empirical Constant	
R_c	Radius of Streamline Curvature	
G	Production Term	
S	Swirl Number	

8. MAILING ADDRESS

Dr. Snehamoy Majumder
Associate Professor
Department of Mechanical Engineering
Jadavpur University, Kolkata
West Bengal, INDIA
PIN- 700032
Phone: 09831369134 (mob)
Email ID: srg_maj@yahoo.com